Journal of Bioenergetics and Biomembranes, Vol. 28, No. 4, 1996

Size and Selectivity of Gap Junction Channels Formed from Different Connexins

Richard D. Veenstra[1]

Received January 7, 1996; accepted February 18, 1996

Gap junction channels have long been viewed as static structures containing a large-diameter, aqueous pore. This pore has a high permeability to hydrophilic molecules of ≈900 daltons in molecular weight and a weak ionic selectivity. The evidence leading to these conclusions is reviewed in the context of more recent observations primarily coming from unitary channel recordings from transfected connexin channels expressed in communication-deficient cell lines. What is emerging is a more diverse view of connexin-specific gap junction channel structure and function where electrical conductance, ionic selectivity, and dye permeability vary by one full order of magnitude or more. Furthermore, the often held contention that channel conductance and ionic or molecular selectivity are inversely proportional is refuted by recent evidence from five distinct connexin channels. The molecular basis for this diversity of channel function remains to be identified for the connexin family of gap junction proteins.

KEY WORDS: Connexin; channel conductance; ionic selectivity; dye permeability; 6-carboxyfluorescein; 2′,7′-dichlorofluorescein; Lucifer Yellow; biionic reversal potentials; conductance ratios; Goldman–Hodgkin–Katz voltage and current equations.

1. INTRODUCTION

The concept of the gap junction channel as a large aqueous pore of 10–14 Å in diameter and only weakly selective among permeant molecules of up to approximately 1 kD in molecular weight has existed in the literature for more than a decade with only slight modification. This means that either the original predictions about the physical dimensions and molecular interactions involved in the permeation process were either extremely accurate or somehow limited in the scope of their observations which have been difficult to overcome over the following years of research. In this minireview, I want to present the essential observations which lead to the development of the long-standing model of the gap junction channel and review recent published observations from my laboratory which have only begun to address this conceptual model in further detail. All of what I am about to discuss would not be possible without the implementation of connexin-specific stable expression strategies and the analytical methods for multichannel statistical analysis of channel recordings which have come about over the last three years.

The prevailing dogma about the molecular permeability limits of the gap junction channel are best summarized by three fluorescent dye transfer studies performed between 1979 and 1981. The first of these investigations utilized a series of lissamine rhodamine B (LRB) or fluorescein isothiocyanate (FITC) peptide conjugates which varied in molecular weight and electronegativity to examine the permeability properties of gap junctions in nine different mammalian cell types and one insect cell line (Flagg-Newton *et al.*, 1979). The fluorescent probes were approximately of constant width (abaxial dimension of 14–16 Å) and gradually increasing length in the molecular weight range of 450–850 daltons. Most notable was the distinction between invertebrate and vertebrate gap junctions since the mammalian cells all exhibited permeability

[1] Department of Pharmacology, SUNY Health Science Center at Syracuse, 750 E. Adams Street, Syracuse, New York 13210.

0145-479X/96/0800-0327$09.50/0

limits using the designed probes mentioned above while the AC-20 insect cell gap junctions passed every probe with relative ease including the 1830-dalton LRB$(PPG)_5OH$ probe. Modest differential permeability limits were also observed among the different mammalian cell lines, ultimately leading to the conclusion that mammalian cell gap junctions vary slightly from each other in a manner consistent with narrower pores and/or increasing electronegativity. This observation of anionic charge associated with gap junction channel pores was quantitatively substantiated by direct measurement of dye permeability in a second invertebrate gap junction, the septal membrane of the earthworm median giant axon (Brink and Dewey, 1980). This study provided the additional observation that a single gap junction can distinguish between fluorescein dye derivatives based primarily on the charge of an associated side chain. There appeared to be significant binding of amino groups while addition of anionic groups (i.e., COOH, Br, Cl) reduced junctional permeability without substantially altering either the molecular weight or width of the molecules. The third defining study used neutral LRB-labeled glycopeptides to probe the pore diameters of two insect cell junctions and three of the original mammalian cell line gap junctions (Schwarzmann *et al.*, 1981). By virtue of exclusion of the smallest impermeant probe, this investigation estimated the limiting pore diameter of the mammalian cell gap junctions to be between 16 and 20 Å while the cutoff for insect cell junctions was between 20 and 30 Å. There are numerous other reports of different tracer molecules being permeable through mammalian gap junctions which are too numerous to mention and have been previously reviewed elsewhere (Imanaga *et al.*, 1987; Brink, 1991). It should also be evident that the larger and more aqueous the diffusion of a molecule through a pore becomes, the more significant the cytoplasmic diffusion becomes in the measurement of actual junctional permeabilities (Brink and Ramanan, 1985; Safranyos *et al.*, 1987; Verselis and Veenstra, 1996). These defining observations contributed significantly to the general understanding of the gap junction channel as a relatively large aqueous pore possessing weak charge selectivity among molecules of $\geq$ 800 daltons and 10–14 Å in width. The one additional parameter to add to this conceptual model of a gap junction channel is that the originally estimated unitary channel conductance of such a channel was 100 pS (Simpson *et al.*, 1977).

If repeated today, these observations in native cell types would likely be faithfully reproduced. What has begun to redefine the conductance and permeability properties of the gap junction are the investigations into the channels formed by distinct connexins. It is these recent observations which will be reviewed subsequently in this article. Finally, these observations will be placed in context of the original permeability studies in native cell cultures and what implications the differing permeability characteristics may have on intercellular communication in the tissues.

2. FUNCTIONAL DIVERSITY AMONG THE CONNEXIN CHANNELS

The first definitive molecular evidence of diversity of gap junctions came from the cloning of distinct gap junction proteins (connexins) from rat liver and heart which provided the cDNA probes for a series of cDNA and genomic cloning studies which have at last count identified twelve different mammalian connexins (Beyer and Willecke, 1996). The first clues as to the functional diversity of the connexins came from expression studies first in oocytes and later in transfected mammalian cell lines (Dahl *et al.*, 1987; Eghbali *et al.*, 1990). The first functional differences to be demonstrated were related to the modulation of junctional conductance by transjunctional (cell-to-cell) voltage differences and the ability to form junctional channels with itself or another connexin, reviewed in an accompanying article (White and Bruzzone) in this series. Evidence as to the disparate channel properties of the different connexins comes from comparisons of single-channel recordings from connexin-transfected mammalian cell pairs (Veenstra *et al.*, 1992). Initially these observations were limited to differences in the unitary conductance properties of each connexin channel.

2.1. Channel Conductance

The unitary conductance values of mammalian gap junction channels was first accomplished in primary cultures of rat lacrimal gland and embryonic chick heart ventricular myocyte cell pairs (Neyton and Trautmann, 1985; Veenstra and DeHaan, 1986). Both values, while slightly different at 120 and 160 pS respectively, were not substantially different from the estimated value as to alter our perception of the gap junction channel pore significantly. Neyton and Trautmann (1985) did perform a few biionic potential exper-

iments that provided direct measurements of relative ion permeabilities for the lacrimal gland gap junction channel (see Section 2.2.2). As cell dissociation and culture procedures have improved, the dual whole cell recording technique has been applied to a wide variety of tissues (reviewed in Verselis and Veenstra, 1996) to the point that little additional information beyond the predominant junctional channel type in a given tissue is provided by this approach today.

The conductance measurements of connexin-specific junctional channels has provided supportive evidence that connexin sequence diversity produces functionally diverse gap junction channels, but provides little direct evidence as to the pore structure and permeability properties beyond the flux per unit time of the major ionic salt contained in the recording pipette. Based on the conceptual model of the gap junction channel as an aqueous cylindrical pore of constant diameter (also known as an "aqueous right cylinder"), estimates of the expected conductance of a channel of increasing diameter under identical ionic conditions can be calculated from a simple equation assuming the channel resistance (1/conductance) is the sum of the pore and access resistances: $R_{channel} = R_{pore} + R_{access} = (\rho l/\pi a^2) + (\rho/2a)$ (Hille, 1992). Assuming a resistivity (ρ) of 100 $\Omega \cdot$ cm and a length (l) of 16 nm, a 100-pS channel has a radius (a) of approximately 7 Å, or pore diameter of 14 Å (Veenstra *et al.*, 1995b). Hence, the initial gap junction channel conductance measurements are within the experimental variation of the original estimates of the channel conductance and diameter.

Of the twelve connexins thus far identified from mammalian tissues, six have been stably transfected and their maximum unitary conductance state determined by conventional junctional channel recording (Verselis and Veenstra, 1996). Under nearly physiological ionic conditions (290 mOsm ± 10%, predominantly KCl), connexin channel conductances range by one full order of magnitude from 30 to 300 pS. Using the above equation, which assumes aqueous conditions and a constant length, one can calculate the range of pore diameters expected for this range of conductances. The estimated pore diameters are a minimum of 8 Å for the connexin45 (Cx45) channel to 24 Å for the human connexin37 (Cx37) channel.

As simple and straightforward as they seem, one could make predictions about the molecular permeability and the ionic selectivity properties of the various connexin channels. Indeed, at least one published account of asymmetric dye transfer has invoked this principle as a means to explain their observation of "preferential directional transfer" of the commonly used fluorescent tracer, Lucifer Yellow CH, between heterotypic cell pairs of astrocytes and oligodendrocytes (Robinson *et al.*, 1993). The term "unidirectional" transfer has been consciously avoided since actual unidirectional (i.e., irreversible) transport of a molecule through an open pore is not thermodynamically possible (Finkelstein, 1994; Meister, 1994; Buehler, 1994). It obviously follows that a higher-conductance channel could more readily pass a molecule with an abaxial dimension of ≈11 Å (e.g., Lucifer Yellow). This concept is a readily testable hypothesis given the ability to inject dyes into whole cell and monitor junctional conductance using dual patch electrodes on connexin-transfected cell pairs. Over the past two years, this laboratory has been actively testing this central hypothesis using two fluorescein dye derivatives, 2′,7′-dichlorofluorescein (diCl-F) and 6-carboxyfluorescein (6-CF), and chloride for glutamate ion substitutions. The following section will summarize the findings of this laboratory as well as others in regard to the selective permeability properties of connexin-specific gap junction channels and how they relate to channel conductance.

2.2. Selective Permeability

The phrase "selective permeability" invokes the use of two determining factors in defining the ability of a particular molecule to pass through a given pore, physical size, and electrostatic charge. As demonstrated by the dye permeability studies of 1979 and 1980, gradually increasing physical size of the fluorescent probe reduces the junctional permeability and increasing the electronegativity of similarly sized probes reduces the junctional permeability even further. Hence, the two variables are integrally related since increasing the molecular dimensions brings existing charges on the molecule into closer proximity to any existing charged amino acid residues associated with the lining of the pore. Electrostatic interactions are but one of a few kinds of intermolecular interactions that can occur between a permeant molecule and the pore wall. Hydrophobic or hydrophilic interactions are also important in determining the free energy of association of a molecule with a particular site in the channel. Hence, the tertiary structure and the chemistry of the exposed residues on the molecule and the pore lining are important determinants of selective perme-

ability. For some ion channels, the space filling model of the minimum pore diameter has been estimated from relative ionic permeability determinations using ions of increasing size or hydration. Often the overall selectivity of an ion channel is determined by highly specific intermolecular interactions at or near the pore diameter restriction site. This site in the channel pore is referred to as the "selectivity filter" and is most likely distinct from other functional domains of the channel protein such as the gate or voltage sensor controlling the open-closed probability of the channel. To date, the selectivity properties and physical dimensions of the selectivity filter of connexin channels have not been determined.

2.2.1. *Molecular Permeability*

The most common assay for gap junctional communication is fluorescent dye transfer using Lucifer Yellow CH, owing to its hydrophilicity and quantum yield (5-fold lower relative to fluorescein, ≈100-fold greater relative to Procion Yellow; Stewart, 1978). Junctional permeabilities can be determined from quantitative imaging of the rate of increase in fluorescence intensity in a non-dye-loaded recipient cell. However, without knowledge of the number of functional channels and their relative conductance state, precise channel permeabilities cannot be determined from such measurements. To ascertain relative permeability differences for connexin channels, the measured junctional permeability should be directly correlated with junctional conductance or, preferably, channel number measurements. Alternatively, relative dye permeabilities of a single connexin channel using dyes of similar axial and abaxial dimensions but different surface charge distributions can provide useful information about the electrostatic interactions involved in pore permeation.

To date two studies have been published which examine the dye permeability of connexin-specific gap junctions in transfected mammalian cells (Elfgang *et al.*, 1995; Veenstra *et al.*, 1995b). The molecular permeability of murine Cx26, Cx31, Cx32, Cx37, Cx40, Cx43, and Cx45 was assessed using five probes of varying physical dimensions and binding properties. Three of the dyes, propidium iodide, ethidium bromide, and DAPI hydrochloride, bind strongly to DNA, which limits their utility as diffusable tracers. Nonetheless, it was demonstrated that all of the connexins were permeable to these cationic dyes with the exception of Cx31 and Cx32. Lucifer Yellow (valence = −2) was readily permeable for all connexins tested. Neurobiotin (287 Da, valence = +1, 5.4 by 12.7 Å) was also demonstrated to be readily permeable for all connexins examined with Cx31 exhibiting the lowest transfer index. This approach clearly demonstrates differential selective permeability for a given dye among the seven connexins examined, but provides no new information about pore size or electronegativity of the channels themselves. Secondly, although junctional conductance (g_j) was determined for the seven transfectants, g_j were ≥ 25 nS on the average, indicating the presence of tens to hundreds of channels for each connexin. Double whole cell patch clamp recordings of junctional currents becomes severely compromised when $g_j \geq$ 25 nS since the average resistance of each patch electrode is ≈20 MΩ or 50 nS (Wang *et al.*, 1992; Veenstra and Brink, 1992). Furthermore, g_j measurements were not obtained in the same cells used for the dye transfer assays, so the actual g_j of the transfering cells is not known.

The experimental approach our lab has taken to address the issue of differential dye permeability of connexin channels varies from the above investigation in two ways (Veenstra *et al.*, 1995b). First, we used two fluorescein derivatives, diCl-F and 6-CF, which varied only in their anionic surface charge distributions (valences = −1 and −2 respectively at pH 7.0). Secondly, 2 mM of either one of these dyes was added directly to one patch pipette during conventional dual whole junctional current recordings thus permitting direct assessment of g_j for each experiment. Stability of g_j over a 10-min observation period was a prerequisite for every experiment. The results of these experiments are illustrated in Fig. 1. The mean $g_j \pm$ standard deviation, and number of cell pairs (n) is plotted for each sample population based on the visual observation of ±dye transfer after 10 min of whole-cell recording. These results indicate that chicken Cx45 (cCx45) can readily distinguish between 6-CF (impermeant) and diCl-F (permeant) over identical g_j ranges, suggesting that electrostatic surface charge plays a significant role in the permeability of this channel to molecules of 9–10 Å in abaxial width. This is clearly not the case for the rat Cx43 channel, where both dyes are 100% permeable. By comparison, 6-CF dye transfer is detectable only when $g_j \geq 4$ nS for chicken Cx43 (cCx43) while diCl-F transfer is detectable even when $g_j = 0.2$ nS. This is consistent with the previous observations of relative dye permeability in the earthworm median giant axon septal membrane (diCl-F > 6-CF ≈ LY

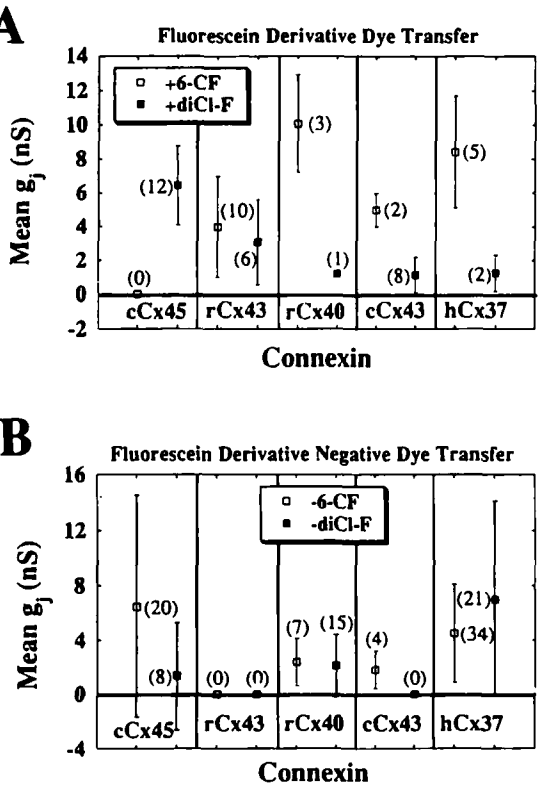

Fig. 1. Correlation of junctional conductance and fluorescein dye transfer. Mean junctional conductance ± standard deviation (g_j ± std) of mouse neuro2A neuroblastoma (N2A) cells transfected with chicken connexin45 (cCx45), rat Cx43 (rCx43), rat Cx40 (rCx40), chicken Cx43 (cCx43), and human Cx37 (Cx37) which were examined for the passage of 2 mM 6-carboxyfluorescein (6-CF; open squares) or 2′,7′-dichlorofluorescein (diCl-F, closed squares). The number of observations for each sample population is given in parentheses. The top panel (A) illustrates the mean g_j of those pairs which exhibited dye transfer after 10 min. The lower panel (B) displays the mean g_j of those pairs where dye transfer was not detectable after 10 min. rCx43 is permeable to both dyes while cCx45 and cCx43 exhibit a higher permeability to diCl-F relative to 6-CF. rCx40 and hCx37 exhibit a low incidence of dye transfer (≤30%) for both dyes. The lower permeability to 6-CF is attributed to its greater anionic charge than diCl-F (valence of −2 and −1, respectively) despite similar abaxial dimensions (≈9.5 Å) and a slightly lower molecular mass for 6-CF(376 daltons and 401 daltons, respectively).

CH; Brink and Dewey, 1980). Rat Cx40 (rCx40) and human Cx37 (hCx37) are only sporadically permeable to both dyes and the incidence of dye transfer is poorly correlated with g_j.

These results are even more surprising when the maximum unitary channel conductances of each connexin in 120 mM K glutamate are taken into consideration. The five connexins are listed in order of increasing channel conductance (left to right) with cCx45 being the smallest at 26 pS, rCx43 = 57 pS, rCx40 = 158 pS, cCx43 = 166 pS, and hCx37 = 295 pS. The channel conductances are not at all useful in predicting the apparent dye transfer of these five connexins, thus providing the first indication that the aqueous right cylindrical model for gap junction channels is not valid for all connexins.

Dye transfer is obviously affected by the channel permeability properties which appear to be different among the seven connexins examined to date. Our observations of hCx37 channel activity also provided evidence that channel open probabilities and conductance states can influence dye transfer (Veenstra *et al.*, 1994). This connexin channel is unique among the seven different connexins we have examined to date by virtue of the dominance of a 70-pS subconductance of the 300-pS main state at low transjunctional voltages (i.e., 25 mV). The main state open probability from our single-channel recordings was also <20% at the same potential, thus making the substate conductance and permeability properties more relevant to the junctional permeability characteristics of this connexin. Unfortunately, it was not possible to determine the relative cationic to anionic permeability characteristics of the Cx37 channel substate. However, in two single-channel experiments in the presence of 2 mM 6-CF a decrease in channel conductance of ≈22% was observed when the polarity of the applied transjunctional voltage facilitated dye transfer (hyperpolarization of the dye-loaded cell) relative to the opposite polarity. What occurs when a transjunctional voltage is applied is that a net junctional current is initiated which consists predominantly of an anionic flux from the relatively hyperpolarized cell and a similar cation flux from the partner cell. When one of the anions is triple the radius of potassium, ion movement likely becomes flux coupled (ion–ion interactions in the pore) and possibly even single file (depending on the pore radius). Based on the differences in Cx37 channel main state conductance in 120 mM KCl, K glutamate, and KCl + 2 mM 6-CF, we estimate the 6-CF aqueous mobility to be <4% relative to glutamate, or ≈0.7% relative to K^+ or Cl^-. Hence, detection becomes a significant factor when using dyes with permeabilities reduced by a factor of 100 relative to KCl, especially when the channel is only open an average of 20% of the time at 25 mV. One can readily predict that the permeability of this same molecule through the substate conducting channel is even lower or absent. The difficulty is that given such low permeabilities to large

molecules, accurate permeability measurements become more difficult to obtain.

2.2.2. *Ionic Permeability*

The above discussion applies to the permeation of large molecules which are presumably approaching the limiting diameter of the pore. Interactions between the pore wall and the permeant molecule are minimized as the relative permeant/pore radii decreases. Such is the case for monovalent anions and cations. Hence, ion selectivity should be less pronounced for larger channels possessing similar electrostatic surface charges. Relative ionic permeabilities have been traditionally determined using asymmetric salts and the constant field voltage (Goldman–Hodgkin–Katz; GHK) equation or from conductance ratio determinations. Measurement of the reversal potential provides a direct determination of the relative permeability values of the two primary ions under biionic (asymmetric) salt conditions. These procedures have been used to determine the specificity of a variety of known ion-selective channels (e.g., Na^+, K^+, Ca^{++}, Cl^-), but have been applied sparingly so far to gap junction channels. Neyton and Trautmann (1985) reported relative permeabilities of 1.0, 0.81, and 0.69 for K^+, Na^+, and Cl^- respectively for the rat lacrimal gland channel. This is the only published report to date using biionic reversal potential measurements to assess the ionic permeability of a gap junction channel. The only other published report of ionic permeability estimates from native gap junction channels comes from Brink and Fan (1989) on the earthworm median giant axon septal membrane channel. Again using asymmetric solutions and determining the reversal potential for the channel, they calculated the conductance ratio of the channel to be 1.0, 1.0, 0.84, 0.64, 0.52, and 0.20 for K^+, Cs^+, Na^+, TMA^+, Cl^-, and TEA^+ (assuming that $G_j = P_j \times K_i \times [F^2/RT]$, where K_i is the intracellular concentration of K^+). Both of these studies demonstrate that Cl^-, which has an aqueous diffusion coefficient of 1.04 relative to K^+, has a reduced permeability (0.62–0.52 relative to K^+) in either of these gap junction channels. This supports the previous conclusion from dye tracer experiments that the gap junction channel has a slight negative charge associated with the pore. The observed ionic selectivity for cations is even weaker than that observed for the only anion, Cl^-, in support of the contention that these two ≈100-pS gap junction channels are only weakly ion selective.

This laboratory sought to investigate the relative anion:cation selectivity of the gap junction channels formed by distinct connexins in order to explore this hypothesis in further detail. Secondly, we chose to relate our findings on the relative anion:cation permeability ratio (R_p value) to the maximum conductance state of the channel to examine the original conception of the gap junction channel as an aqueous right cylinder where conductance is a function of pore radius and inversely proportional to selectivity (Section 2.1). To accomplish this, we performed equimolar (120 mM) Cl^- for glutamate substitutions and measured the change in single-channel conductance (γ_j) of each connexin channel expressed in the N2A cell line using conventional dual whole cell junctional recording techniques. Owing to the difficulty of internally perfusing each pipette, we chose to make repeated measurements of γ_j for each connexin channel in both KCl and K glutamate pipette solutions. In all cases, γ_j was taken as the slope conductance obtained from linear regression of the single-channel junctional current–voltage relationship for each experiment. Estimation of the R_p value depended upon the relative increase in γ_j under experimental conditions to the theoretical increase in γ_j expected for an entirely aqueous pore as determined from the Goldman–Hodgkin–Katz (GHK) current equation (Hille, 1992):

$$I_s = \sum_{s=0}^{i} P_s z_s^2 \frac{EF^2[S]_1 - [S]_2 \exp(z_s FE/RT)}{1 - \exp(-z_s FE/RT)}$$

where I_s is the current carried by each ion s, $[S]$ is the solute concentration on each side of the channel, z is the valence of each ion, F is Faraday's constant, E is the (transjunctional) voltage gradient, R is the gas constant, T is the absolute temperature (°K), and P_s is the permeability of ion s. P_s; eq $D_s\beta_s/l = RT\mu_s\beta_s/Fl \approx K_s\mu_s$, where D_s is the aqueous diffusion coefficient, β_s (=1) is the partition coefficient, l is the channel length, K_s is a constant ($RT\beta_s/Fl$), and μ_s is the aqueous mobility of each ion s. From this equation a 49% increase in current is expected for an aqueous channel with no ionic selectivity of its own when Cl^- is substituted for glutamate$^-$. These calculations are based on the aqueous diffusion coefficients of K^+, Na^+, Cs^+, TEA^+, Cl^-, and glutamate$^-$ (at 25°C: 1.96, 1.33, 2.06, 0.87, 2.03, and 0.39). Since only the anions are being substituted, it follows that the experimental KCl/K glutamate γ_j ratio is <1 if the channel favors cations and >1 if the channel favors anions.

In a series of experiments, the KCl/K glutamate γ_j ratio was determined for seven distinct connexin

channels. These values were: chicken Cx45, 1.23 (=32/26 pS) (theoretical ratio = 1.74 since a different K glutamate solution was used); rat Cx43, 1.40 (=80/57 pS); rat Cx40, 1.14 (=180/158 pS); chicken Cx43, 1.19 (=198/166 pS); human Cx37, 1.36 (=347/295 pS); rat Cx26, 1.22 (=135/110 pS); and rat Cx32, 1.51 (=53/35 pS) (Veenstra *et al.*, 1995b; Suchyna *et al.*, 1994). To estimate the R_p value for each connexin, channel, we modified the GHK current equation as follows:

$$I_s = \sum_{s=0}^{c} P_s z_s^2 \frac{EF^2[S]_1 - [S]_2 \exp(-z_s FE/RT)}{1 - \exp(-z_s FE/RT)}$$

$$+ R_p \sum_{s=0}^{a} P_s z_s^2 \frac{EF^2[S]_1 - [S]_2 \exp(-z_s FE/RT)}{1 - \exp(-z_s FE/RT)}$$

where the original equation has now been divided into separate cationic (c) and anionic (a) components and R_p is expressed as a scaling factor applied to the anionic permeability term of the equation. Using this expression and the experimentally determined KCl/K glutamate γ_j ratios, we determined the R_p value for each connexin channel by scaling it from an original value of 1 to a final value which provided the exact solution to the experimental γ_j ratio. The R_p value of each connexin channel was: cCx45k, 0.10; rCx43, 0.77; rCx40, 0.22; cCx43, 0.32; hCx37, 0.29; rCx26, 0.38; and rCx32, 1.06 (Veenstra *et al.*, 1995b). The log of these R_p values are plotted versus γ_j (in K glutamate) in Fig. 2. It is immediately obvious that selectivity even at the ionic level does not have any correlation to γ_j. These results are in contradiction to the commonly held conceptual model of the gap junction channel. At the same time, these results are consistent with the previous conclusion that the pores are slightly anionic since all connexin channels examined so far exhibit some degree of cation selectivity (0.77–0.10) with the exception of rCx32. These results are also consistent with the observed incidence of dye transfer for five of the seven connexins thus far examined. Hence, the connexin family of channels exhibits a range of anion:cation selectivities from 1:1 to 1:10. This indicates that there is more diversity of function than previously attributed to gap junction channels, although the relative selectivities are considerably less than that observed for the membrane voltage-gated ion channels (Na^+, K^+, Ca^{++}). From this observation, we concluded that weak electrostatic fields could be the determining factor in connexin-specific gap junction channel permeability. Since the effect of a fixed electrostatic field diminishes as a function of distance from

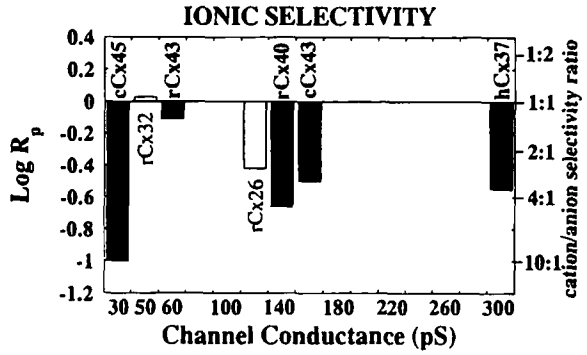

Fig. 2. Semilog plot of the R_p values and channel conductance of seven connexin channels expressed in N2A cells. The log of the R_p value for each connexin channel examined thus far (r = rat, c = chicken, h = human) is plotted as a function of the maximum unitary conductance in symmetrical K glutamate internal pipette solutions. For comparison, the equivalent for the corresponding cation-to-anion selectivity ratio is given on the right axis. All data are modified from Veenstra *et al.* (1995) based on the subsequent experimental determination of the aqueous glutamate mobility with the exceptions of rCx26 and rCx32 which have previously appeared only in abstract form (Suchyna *et al.*, 1994).

the pore wall and increasing ionic strength, ionic conditions and pore diameter will also be relevant variables to examine experimentally.

Presently, this laboratory is performing more extensive cation and anion conductance ratio sequences to examine the ionic selectivity of connexin-specific channels in greater detail. As part of these ongoing investigations, we are performing asymmetric ionic salt (115 mM K^+Y^- or X^+Cl^-) substitutions on the transfected rat Cx43 and Cx40 gap junction channels expressed in N2A cells for comparison of the aqueous mobility, channel conductance, and relative permeability sequences to permit a more detailed comparison of the distinct permeabilities and aqueous nature of the respective channel pores (Beblo *et al.*, 1994; Wang and Veenstra, 1995).

2.3. Estimation of Pore Size

Information about relative pore sizes is best obtained using conjugated fluorescent probes or other probes (e.g., sugar moieties) which rely on the exclusion of the smallest impermeant molecule. As observed in the previous section, pore diameter can directly affect ionic permeability depending on the relative strength of the electrostatic surface charge of the pore and the distance to the permeant ion or molecule.

Hence, precise determination of pore diameters will directly aid investigators in constructing more detailed models of connexon pores. The approximate physical dimensions of the selectivity filters of several ion-selective voltage-gated and ligand-gated channels have been exquisitely determined using organic anions and cations of increasing size but equal valence (for review, see Hille, 1992). The dye permeation studies performed over a decade ago perform a similar task, but they are unfortunately lacking in the Å resolution and pA sensitivity that electrical channel recordings can provide.

Most estimates of pore size depend on the relative dimensions of the permeant molecule and the measurement of the current it is capable of carrying. In a few instances, the sequences which form the selectivity filters' electrostatic components and physical constraints have been directly examined by site-directed mutagenesis. One channel which possesses some similarities to the gap junction channels is the nicotinic acetylcholine receptor (AChR) channel. This heteropentameric ($\alpha\beta\alpha\gamma\delta$ subunits) channel is a cation-selective channel with a selectivity filter of 6.5 Å by 6.5 Å and the pore is formed by an amphipathic α-helix (Dwyer *et al.*, 1980; Mishina *et al.*, 1985; Imoto *et al.*,, 1986). Some of the earliest site-directed mutagenesis studies identified three anionic rings of charge, one located near each opening of the channel and one located $\approx 1/3$ of the pore length from the cytoplasmic opening of the channel (Imoto *et al.*, 1988). Altering the negative charge by substitution of neutral or basic amino acids at any of these sites reduced the conductance and Mg^{++}-dependent block of the AChR channel. The innermost ring had the most dramatic effect on channel conductance and was assumed to be located at the narrowest part of the pore. This model has been subsequently revised by the demonstration that the adjacent inner ring of the M2 α-helix, containing mostly uncharged polar (serine and threonine) or nonpolar (glycine) amino acid residues, forms the narrowest part of the pore and contributes significantly to its selective permeability (Villarroel *et al.*, 1992; Villarroel and Sakmann, 1992). The final demonstration of this model comes from mutagenesis experiments performed on the "central" ring of the AChR channel where key residues were mutated to similar residues having side chains with different volumes, thus narrowing or widening the selectivity filter for the channel (Villaroel *et al.*, 1992; Villaroel and Sakmann, 1992; Wang and Imoto, 1992). This is the most elegant study of the structure–function of a channel's selectivity filter and demonstrates that the electrostatic and physical constraints placed on the permeant ions do not necessarily reside on the same residues lining the pore, but may be located on spatially juxtaposed amino acid residues. The development of the model for this channel has also been aided significantly by three-dimensional analysis of the AChR tertiary structure (Unwin, 1993).

A principal element in this analysis of function is the determination of biionic permeability ratios and relating them to their respective volumes or, conversely in the case of amino acid substitutions, the volumes of the amino acid side chains. To accomplish this requires modeling the volume of the ion or amino acid in three dimensions. Secondly, the viscous drag of the solvent space within the pore upon the permeant molecule is believed to create a frictional force opposing its diffusion equal to the hydrodynamic equations used to calculate a ball falling through a homogeneous viscous medium in a cylinder. Various functions incorporating both volume and viscous drag effects have been formulated to better model the permeation of a molecule through a pore, although none precisely define the organic cation permeability of the frog end plate AChR channel (Renkin, 1955; Levitt, 1975; Dwyer *et al.*, 1980). The cation and anion conductance and permeability ratio sequences presently being performed on two connexin-containing channels are yielding enough information to estimate connexon pore diameters by employing the hydrodynamic principles outlined above (Veenstra *et al.*, 1995a). Not surprisingly, these initial determinations are already indicating that pore diameters vary significantly among homotypic connexon channels.

3. MOLECULAR BASIS FOR FUNCTIONAL DIVERSITY

As observed from the previous section, there is an obvious advantage to having identified the amino acid sequences which determine the permeability characteristics of a given pore. Not only does the necessary permeability properties of a given connexin channel remain to be provided in sufficient detail, but determination of a pore-forming sequence for the connexins also remains to be experimentally verified. There are two alternative hypotheses which appear in the present gap junction literature which, by virtue of their relative acceptance in the gap junction field, merit further consideration here.

The more common hypothesis for the pore-forming segment of the connexin family of gap junction proteins is the "M3 hypothesis" which has already received enough consideration to appear in two previous reviews on gap junctions (Bennett *et al.*, 1991; Willecke *et al.*, 1991). "M3" stands for the third transmembrane domain of all connexins and is, by virtue of its primary amino acid sequence, presumed to be the most amphipathic α-helix of the four conserved transmembrane domains of the connexins. Hence, I will not repeat the observations presented in these reviews, but I will examine the experimental conductance and permeability data that addresses this hypothesis.

There exist only two reports in the gap junction literature of alterations in channel conductance or permeability properties following site-directed mutagenesis. Both observations were made using human Cx43 transfectants and involved two different domains, the cytoplasmic tail and M3. In the first study, truncation of the last 80 or 138 amino acids from the carboxyl terminal tail of hCx43 resulted in apparent alterations in γ_j compared to the wild-type hCx43 (Fishman *et al.*, 1991). The shorter (80 aa) truncation mutant reportedly produced a 160-pS channel compared to the two conductance states observed in the wild type channel of 100 and 60 pS. The second longer (138 aa) truncation mutant had the opposite effect of lowering the channel conductance to 50 pS. It should be noted that these unitary events were obtained in the presence of 1.5–2.0 mM halothane, and conductance measurements were made from a single-event amplitude histogram consisting of at most 382 channel events obtained from eight cell pairs containing the wild type channel. The mutant γ_j data came from only two cell pairs and 178 or 132 channel events respectively. Hence, the reliability of the results is not as well documented as other examples using *I–V* relations constructed from long duration pulses to multiple transjunctional potentials in the absence of pharmacological interventions. No information about the permeability of these mutant channels was provided. From this observation, the authors contend that the carboxyl terminus plays an important role in defining the conductance properties of the connexin channel.

The second investigation observed the reduction of Lucifer Yellow dye transfer in a mutant hCx43 channel where serine 158 (S158) in the M3 domain was mutated to either a phenylalanine (P), lysine (K), or aspartic acid (D) residue (Spray *et al.*, 1992). In all three cases, electrical coupling was evident although the γ_j values were not provided except for the statement that in the S158K mutant, γ_j was higher than in the wild type hCx43. No supportive evidence was published in this minicommunication nor have these observations been published in full elsewhere. Also, no selective permeability data has been provided since this preliminary observation was reported. Nonetheless, the authors suggest this experiment supports the contention that M3 is the pore-forming domain. Further experimentation (conductance and permeability ratios) is merited to document this conclusion. Furthermore, the authors make no attempt to relate the two independent findings of the carboxyl tail and the S158 mutant channels as to how they might be influencing channel conductance and permeability properties.

The only true permeability data on gap junction channels comes from the biionic and equimolar anion and cation substitution experiments reviewed above (Section 2.2.2). In the case of the native channels, the connexins involved were not identified. One perhaps startling observation from Veenstra *et al.* (1995b) is the twofold difference in γ_j and R_p values between rat and chick Cx43, with cCx43 being higher in both γ_j and ionic selectivity (lower R_p). The M3 domains of rCx43 and cCx43 are identical (GGLLRTYIISILFKS-V(I)FEVAFLLIQ) and hCx43 varies by only one residue (V164I, in parentheses). This observation does not preclude the hypothesis that the M3 domain lines the transmembrane portion of the pore, but it does dispute the concept that any part of this sequence is relevant to determining the selectivity filter of the connexon pore.

A more recent hypothesis that has received considerably less attention than the M3 hypothesis is the result of the rCx32 synthetic peptide sequence experiments of Dahl *et al.* (1994). A single dodecapeptide (E2a) corresponding to part of the second extracellular (E2) loop of Cx32 was found to produce a membrane conductance when reconstituted into artificial lipid bilayers, presumably in a single (i.e., hemichannel) configuration. Other dodecapeptides representing partial E1 or E2 sequences failed to induce a membrane conductance and longer E2 peptides which included only the last four amino acids of the E2a peptide also failed to produce any bilayer conductance. The question that remains is if longer sequences containing this 12-mer can induce a membrane conductance since the role of this partial sequence in the intact connexin protein remains unknown. If true, such information would substantiate the role of this domain in the intact connexin protein. The model is intriguing since the E2a peptide sequence (residues 156–167, LYPGY-

AMVRLVK) is located near the carboxyl end of M3. However, essentially all of the evidence that M3 and E2a contribute to the pore lining is based on correlations drawn from other ion channels where an amphipathic α-helical transmembrane domain (e.g., AChR) or extracellular linker domain dips into the membrane in a presumed β-strand conformation (e.g., voltage-gated Na^+, K^+, Ca^{++}) to form the pore. There is no direct evidence to support these contentions for the connexin channels while the formative experiments have already been performed and examined by site-directed mutagenesis for the other channels from which these analogies have been drawn. Secondly, the initial estimates as to the location of the pore-forming domains of the AChR channel based on hydropathy plot analyses (Mishina *et al.*, 1985) were later proven to be incorrect by observations which accurately defined the pore-forming segments (Imoto *et al.*, 1986). Hence, there is no substitute for performing current–voltage relations and permeability ratio experiments in combination with domain swapping and site-directed mutagenesis to document the effects on the conductance and permeability properties of the channel under investigation to definitively identify its pore-forming domain. Presently, there is not enough information on the connexin channels to make similar conclusions from the limited number of mutagenesis studies performed to date.

4. PHYSIOLOGICAL CONSEQUENCES OF DIVERSITY OF CHANNEL FUNCTION

Since the major function of the connexin is to form an intercellular channel capable of electrical and chemical signaling required to maintain tissue homeostasis and promote cell-to-cell signal transduction, what do these new observations imply in terms of physiologically relevant electrical and chemical signaling? Since all of the connexin channels examined are capable of establishing electrical communication and demonstrate a finite permeability to K^+, all connexins are capable of supporting electrical communication with only the rates of cation and anion fluxes being different among them. Of probably greater significance is the differential permeability to tracer molecules having permeabilities similar to relevant second messengers such as 1,4,5-inositol trisphosphate (IP_3) or Ca^{++} and 3′,5′-cyclic adenosine monophosphate (cAMP). Presently, we can only make predictions about which connexin channels may pass these important second messengers. It is rather obvious from the molecular and ion selectivity experiments performed thus far that the Cx43 channel is quite capable of promoting intercellular signal transduction by the diffusion of anionic molecules as large as cAMP or IP_3. Since Cx43 is expressed in a wide variety of epithelial, connective, and muscle tissues, this observation may explain many of the early defining permeability studies on mammalian gap junction channels. If the presence of Cx43 channels in significant abundance imparts molecular permeability properties consistent with the early dye tracer studies of a decade ago on the tissues where they are expressed, what implication does the expression of these other less permeable connexins have on the native cell types? Ultimately, this question will have to be addressed in multiple connexin expression systems or the native cells under conditions which allow the investigator to selectively modulate the different connexin channels. Another possibility is that coexpression of connexins leads to formation of mixed connexin hemichannels (heteromeric channels) or heterotypic (homomeric hemichannels formed by unlike connexins) between cells which may alter the conductance and selectivity properties in unique ways (i.e., rectification by preferential directional permeability or gating). These possibilities are only beginning to be explored using the connexin-specific expression systems presently available.

5. FUTURE DIRECTIONS

Future investigations are likely to focus on the questions raised by these most recent observations outlined in this minireview. Based on knowledge gained so far and to be attained in the coming year, we can formulate more definitively testable hypotheses about connexin channel permeability and devise new experiments to test the hypotheses that there are differential second messenger permeabilities to gap junction channels. Some heterotypic junctions will likely preferentially alter intercellular diffusion enough to form gradients of cytoplasmic diffusable molecules (e.g., ions, second messengers, morphogens). Heteromeric channels may similarly alter the conductance, permeability, and gating properties of gap junction channels to form another functionally unique population of channels. Defining functional domains within the connexin family of proteins will continue to be active area of investigation as it has been primarily in the oocyte expression system to

date, with obvious advantages of extending these to the transfection expression systems from which the connexin channel literature has been derived. Some of this work is already commencing. Ultimately, the theories formulated in these *in vitro* expression systems will have to be applied to native cells *in vitro*, or even better *in vivo*, to determine the actual physiological consequences of these differential channel populations and their respective permeabilities.

ACKNOWLEDGMENTS

The Cx43, Cx45, Cx40, and Cx37 transfected N2A cells were provided by Ms. Eileen Westphale and Dr. Eric C. Beyer of Washington University, St. Louis, Missouri. The experiments on these cloned connexins were performed by Drs. Hong-Zhan Wang and Dolores A. Beblo in my laboratory. Cx26 and Cx32 transfected N2A cells were prepared by Dr. Bruce J. Nicholsons' laboratory and the electrophysiogical recordings were performed by Dr. Tom Suchyna while visiting my laboratory. I wish to thank Drs. Peter R. Brink and Andrew Harris for many helpful discussions on the permeability properties of membrane channels. All N2A cell cultures were maintained by Mr. Mark Chilton. This work was supported by NIH grants HL-42220 and HL-45466 and an Established Investigatorship Award from the American Heart Association.

REFERENCES

Beblo, D. A., Wang, H.-Z., Westphale, E. M., Beyer, E. C., and Veenstra, R. D. (1994). *Circulation* **90**, I-359.

Bennett, M. V. L., Barrio, L. C., Bargiello, T. A., Spray, D. C., Hertzberg, E., and Saez, J. C. (1991). *Neuron* **6**, 305–320.

Beyer, E. C., and Willecke, K. (1996). In *Advances in Molecular and Cell Biology*, Vol. 18 (Hertzberg, E. L., ed.), JAI Press, Greenwich, Connecticut, in press.

Brink, P. R. (1991). *J. Cardiovasc. Electrophysiol.* **2**, 360–366.

Brink, P. R., and Dewey, M. M. (1980). *Nature* **285**, 101–102.

Brink, P. R., and Fan, S.-F. (1989). *Biophys. J.* **56**, 579–593.

Brink, P. R., and Ramanan, S. V. (1985). *Biophys. J.* **48**, 299–309.

Buehler, L. (1994). *Science* **265**, 1018–1019.

Dahl, G., Miller, T., Paul, D., Voellmy, R., Werner, R. (1987). *Science* **236**, 1290–1293.

Dahl, G., Nonner, W., and Werner, R. (1994). *Biophys. J.* **67**, 1816–1822.

Dwyer, T. M., Adams, D. J., and Hille, B. (1980). *J. Gen. Physiol.* **75**, 469–492.

Eghbali, J., Kessler, A., and Spray, D. C. (1990). *Proc. Natl. Acad. Sci. USA* **87**, 1328–1331.

Elfgang, C., Eckert, R., Lichtenberg-Fraté, H., Butterweck, A., Traub, O., Klein, R. A., Hülser, D. F., and Willecke, K. (1995). *J. Cell Biol.* **129**, 805–817.

Finkelstein, A. (1994). *Science* **265**, 1017–1018.

Fishman, G. I., Spray, D. C., and Leinwand, L. A. (1990). *J. Cell Biol.* **111**, 589–598.

Fishman, G. I., Moreno, A. P., Spray, D. C., and Leinwand, L. A. (1991). *Proc. Natl. Acad. Sci. USA* **88**, 3525–3529.

Flagg-Newton, J., Simpson, I., and Loewenstein, W. R. (1979). *Science* **205**, 404–407.

Hille, B. (1992). *Ionic Channels of Excitable Membranes*, Sinauer Associates Inc., Sunderland, Massachusetts.

Imanaga, I., Kameyama, M., and Irisawa, H. (1987). *Am. J. Physiol. (Heart Circ. Physiol. 21)* **252**, H223–H232.

Imoto, K., Busch, C., Sakmann, B., Mishina, M., Konno, T., Nakai, J., Bujo, H., Mori, Y., Fukuda, K., and Numa, S. (1988). *Nature* **335**, 645–648.

Imoto, K., Methfessel, C., Sakmann, B., Mishina, M., Mori, Y., Konno, T., Fukuda, K., Kurasaki, M., Bujo, H., Fujita, Y., and Numa, S. (1986). *Nature* **324**, 670–674.

Levitt, D. G. (1975). *Biophys. J.* **15**, 533–551.

Meister, M. (1994). *Science* **265**, 1018.

Mishina, M., Tobimatsu, T., Imoto, K., Tanaka, K.-i., Fujita, Y., Fuduka, K., Kurasaki, M., Takahashi, H., Morimoto, Y., Hirose, T., Inayama, S., Takahashi, T., Kuno, M., and Numa, S. (1985). *Nature* **313**, 364–369.

Neyton, J., and Trautmann, A. (1985). *Nature* **317**, 331–335.

Renkin, E. M. (1955). *J. Gen. Physiol.* **38**, 225–243.

Robinson, S. R., Hampson, E. C. G. M., Munro, M. N., and Vaney, D. I. (1993). *Science* **262**, 1072–1074.

Safranyos, R. G. A., Caveney, S., Miller, J. G., and Peterson, N. O. (1987). *Proc. Natl. Acad. Sci. USA* **84**, 2272–2276.

Schwarzmann, G., Weingandt, H., Rose, B., Zimmermann, A., Ben-Haim, D., and Loewenstein, W. R. (1981). *Science* **213**, 551–553.

Simpson, I., Rose, B., and Loewenstein, W. R. (1977). *Science* **195**, 294–296.

Spray, D. C., Moreno, A. P., Eghbali, B., Chanson, M., and Fishman, G. I. (1992). *Biophys. J.* **62**, 48–50.

Stewart, W. W. (1978). *Cell* **14**, 741–759.

Suchyna, T. M., Veenstra, R. D., Chilton, M., and Nicholson, B. J. (1994). *Mol. Biol. Cell* **5**, 199a.

Unwin, N. (1993). *J. Mol. Biol.* **229**, 1101–1124.

Veenstra, R. D., and Brink, P. R. (1992). In *Cell–Cell Interactions: A Practical Approach* (Stevenson, B. R., Gallin, W. J., and Paul, D. L., eds.), IRL Press, Oxford, UK, pp. 167–201.

Veenstra, R. D., and DeHaan, R. L. (1986). *Science* **233**, 972–974.

Veenstra, R. D., Wang, H.-Z., Westphale, E. M., and Beyer, E. C. (1992). *Circ. Res.* **71**, 1277–1283.

Veenstra, R. D., Wang, H,-Z., Beyer, E. C., Ramanan, S. V., and Brink, P. R. (1994). *Biophys. J.* **68**, 1915–1928.

Veenstra, R. D., Beblo, D. A., Wang, H.-Z., and Brink, P. R. (1995a). *Mol. Biol. Cell* **6**, 190a.

Veenstra, R. D., Wang, H.-Z., Beblo, D. A., Chilton, M. G., Harris, A. L., Beyer, E. C., and Brink, P. R. (1995b) *Circ. Res.* **77**, 1156–1165.

Verselis, V. K., and Veenstra, R. D. (1996). In *Advances in Molecular and Cell Biology*, Vol. 18 (Hertzberg, E. L., ed.), JAI Press, Greenwich, Connecticut, in press.

Villaroel, A., and Sakmann, B. (1992). *Biophys. J.* **62**, 196–205.

Villaroel, A., Herlitze, S., Witzemann, V. Koenen, M., and Sakmann, B. (1992). *Proc. R. Soc. London B* **249**, 317–324.

Wang, F., and Imoto, K. (1992). *Proc. R. Soc. London B* **250**, 11–17.

Wang, H.-Z., and Veenstra, R. D. (1995). *Circulation* **92**, I–40.

Wang, H.-Z., Li, J., Lemanski, L. F., and Veenstra, R. D. (1992). *Biophys. J.* **63**, 139–151.

Willecke, K., Hennemann, H., Dahl, E., Jungbluth, S., and Heynkes, R. (1991). *Eur. J. Cell Biol.* **56**, 1–7.